

## Electronic Supplementary Information

# Soft Janus particles: Ideal building blocks for template-free fabrication of two-dimensional exotic nanostructures

Zhan-Wei Li,<sup>†</sup> Zhong-Yuan Lu,<sup>‡</sup> and Zhao-Yan Sun<sup>\*,†</sup>

*State Key Laboratory of Polymer Physics and Chemistry, Changchun Institute of Applied  
Chemistry, Chinese Academy of Sciences, Changchun 130022, China, and Institute of Theoretical  
Chemistry, State Key Laboratory of Theoretical and Computational Chemistry, Jilin University,  
Changchun 130023, China*

E-mail: zysun@ciac.ac.cn

---

\*To whom correspondence should be addressed

<sup>†</sup>Changchun Institute of Applied Chemistry

<sup>‡</sup>Jilin University

Table S1: The corresponding relation<sup>1</sup> between the strength of attraction  $\alpha_{11}^A$  and the range of attraction  $\delta$  or the adhesion energy  $G$  when  $\alpha_{11}^R = 396$ . In the simulations, increasing  $\alpha_{11}^A$  corresponds to the increase of the adhesion energy  $G$  in a reasonable range from  $1.18 k_B T$  to  $18.75 k_B T$ , which may represent hydrophobic or hydrogen bond interactions between attractive middle bands, and can also be tuned by altering salt concentration, pH, or temperature in experiments. The range of attraction  $\delta$  will also gradually increase because of the deformability of soft Janus particles. The parameters  $\alpha_{11}^R$ ,  $\alpha_{11}^A$ , and  $\delta$  are given in reduced units.

$G [k_B T]$	$\alpha_{11}^R$	$\alpha_{11}^A$	$\delta$
1.18	396	66	0.08
2.00	396	88	0.10
2.99	396	110	0.12
4.13	396	132	0.14
5.39	396	154	0.16
6.77	396	176	0.18
7.50	396	198	0.20
9.82	396	220	0.22
11.47	396	242	0.23
13.20	396	264	0.25
14.99	396	286	0.27
16.84	396	308	0.28
18.75	396	330	0.29

## References

- (1) Z.-W. Li, Z.-Y. Lu, Z.-Y. Sun and L.-J. An, *Soft Matter*, 2012, **8**, 6693.

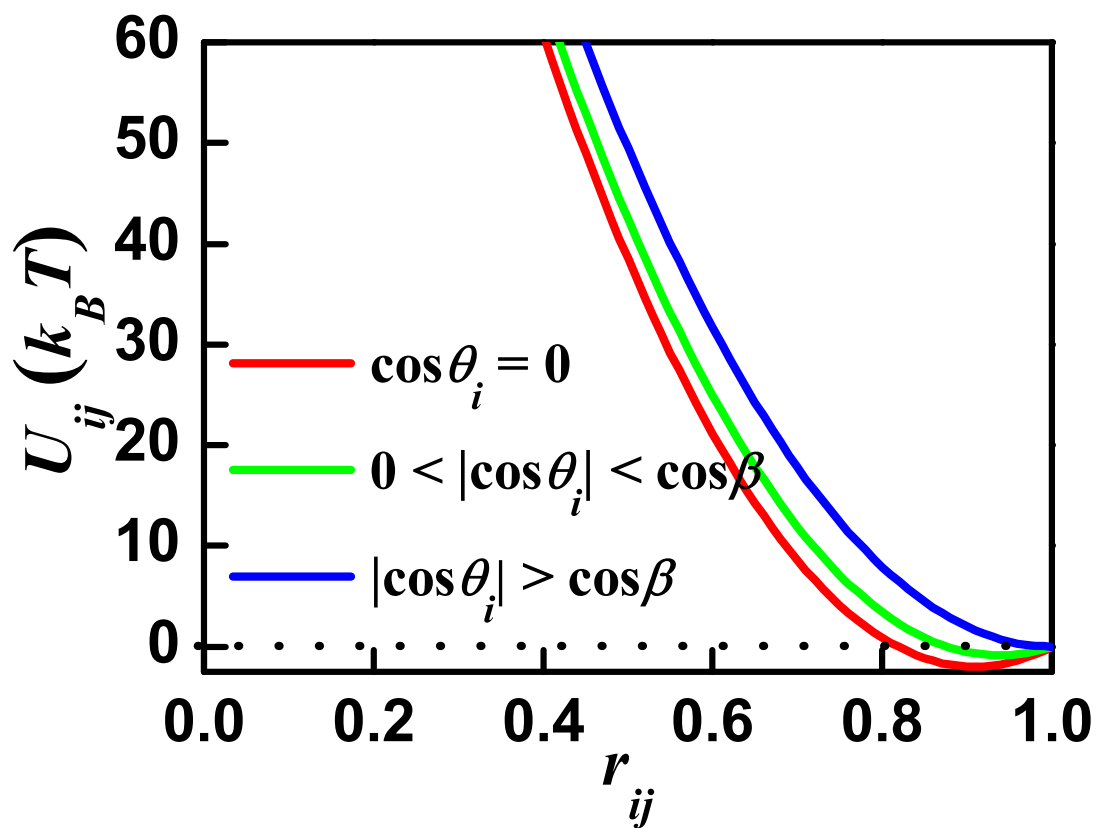


Figure S1: Distance dependence of the anisotropic attractive potential  $U_{ij}$  for different  $\theta_i$ . In this figure, we choose  $\alpha_{ij}^R = 396$ ,  $\alpha_{ij}^A = 88$ ,  $\nu = 1/2$ , and  $\theta_j = 90^\circ$ .

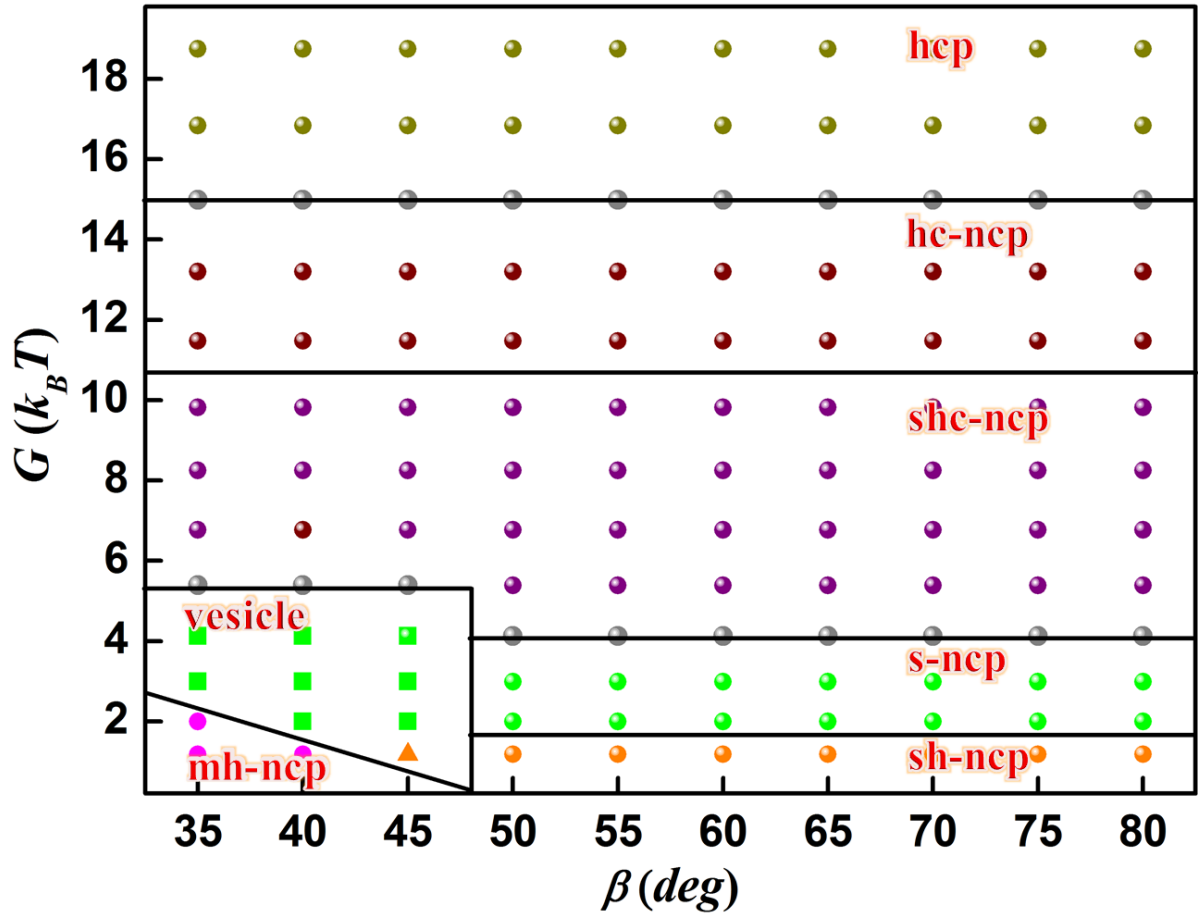


Figure S2: (a) Self-assembly diagram of soft triblock Janus particles in the  $G - \beta$  plane, different colored symbols refer to the simulation results, phase boundaries are drawn schematically to guide the eyes. The gray symbols represent the coexisting structures of s-ncp arrays and shc-ncp arrays, and the coexisting structures of hc-ncp arrays and hcp arrays, respectively.

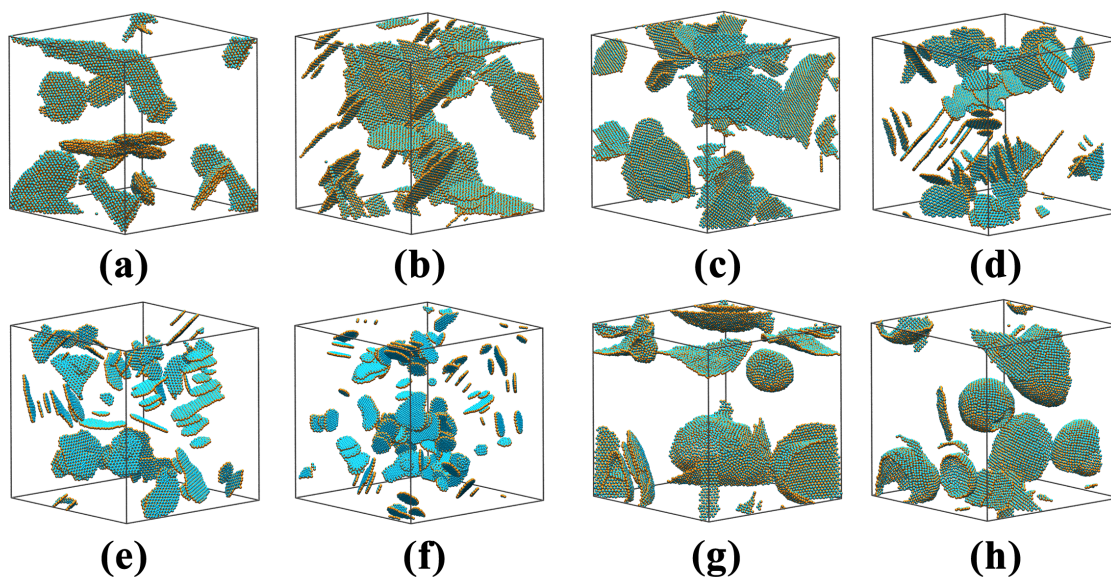


Figure S3: The self-assembled nanostructures for larger system size of  $1.92 \times 10^5$  particles in a  $40 \times 40 \times 40$  cubic box: (a) multi-layer hexagonal ncp (mh-ncp) arrays, (b) 2D single-layer hexagonal ncp (sh-ncp) arrays, (c) square ncp (s-ncp) arrays, (d) stretched honeycomb-like ncp (shc-ncp) arrays, (e) honeycomb-like ncp (hc-ncp) arrays, (f) hcp arrays, and the vesicles with the hexagonal (g) and square (h) ncp surface lattices. For the sake of clarity, we only show Janus solute particles in these systems.

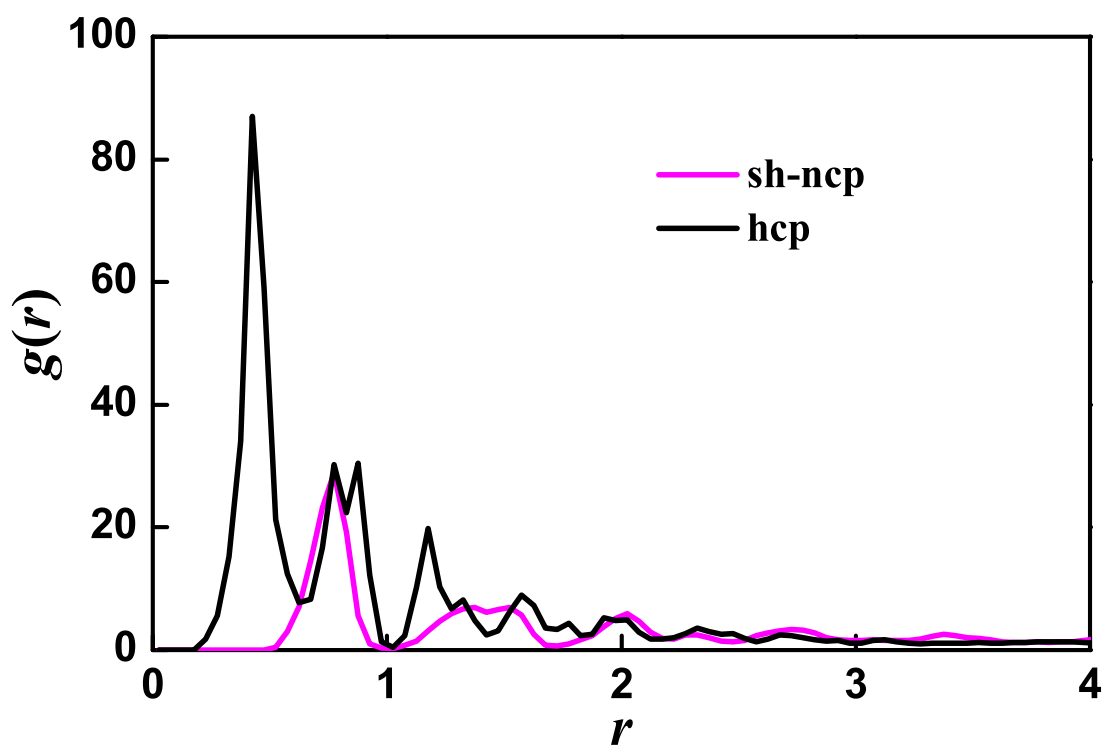


Figure S4: The comparison of the radial distribution functions  $g(r)$  of 2D single-layer hexagonal ncp (sh-ncp) arrays and hcp arrays.

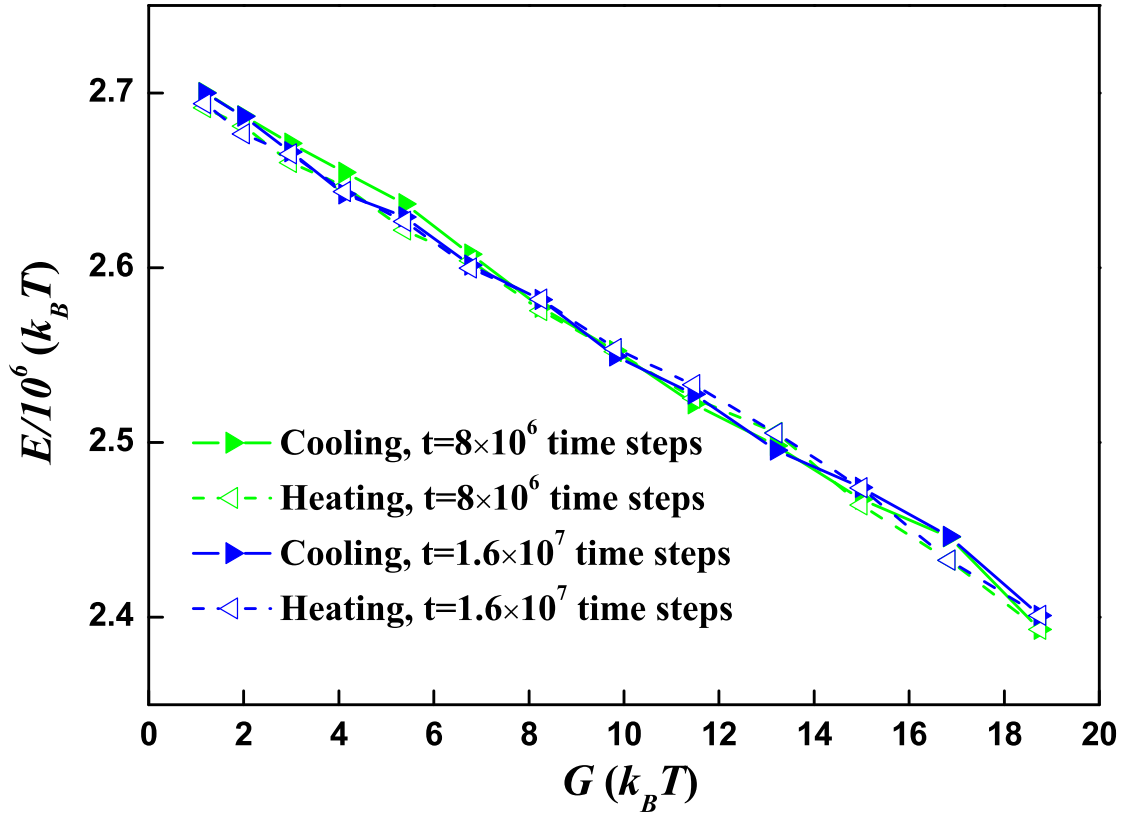


Figure S5: The potential energy  $E$  versus the adhesion energy  $G$ , the triangle solid symbols represent the energies obtained on cooling and the triangle open symbols represent those obtained on heating. The annealing-like processes are reversible because of almost no discontinuity and hysteresis.

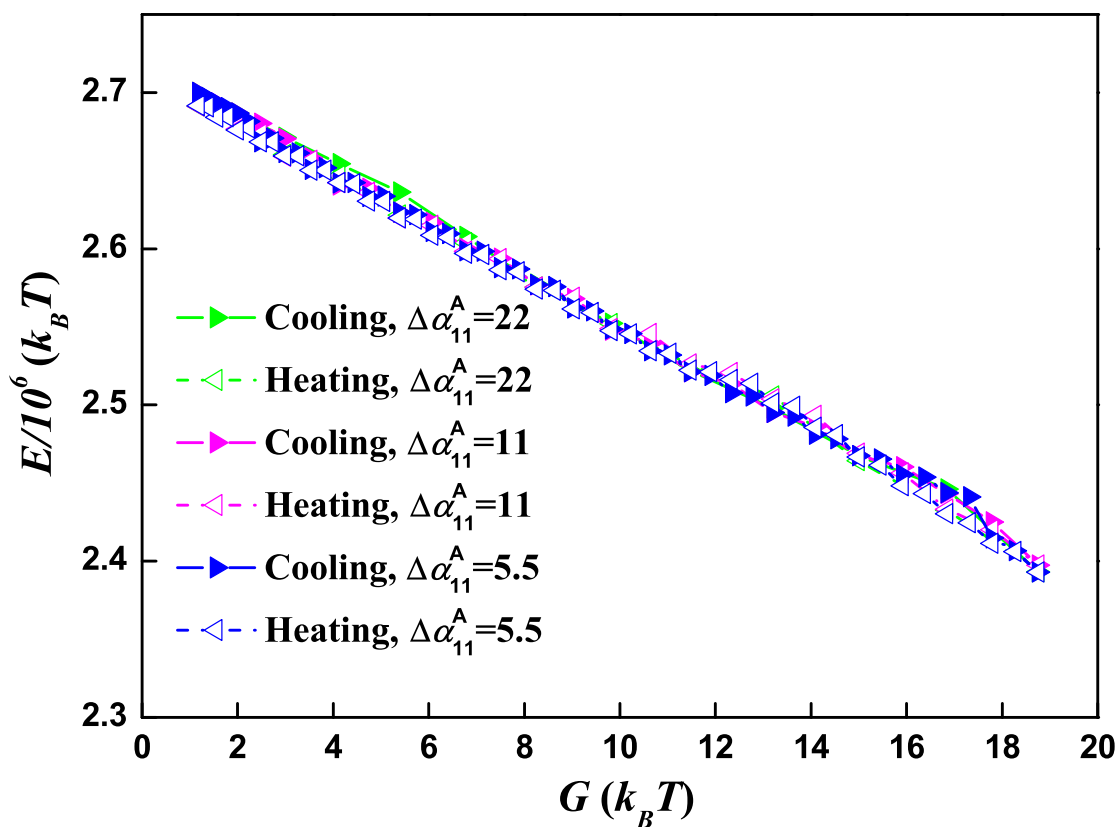


Figure S6: The potential energy  $E$  versus the adhesion energy  $G$  at different cooling and heating rates (i.e. different  $\Delta\alpha_{11}^A$ ), the triangle solid symbols represent the energies obtained on cooling and the triangle open symbols represent those obtained on heating. These annealing-like processes start from the 2D hexagonal ncp nanostructures. It should be noted that the curves for different cooling and heating rates are almost overlapping, which implies that these annealing-like processes are all reversible.